Conductivity Enhancement Mechanism of the Poly(ethylene oxide)/Modified-Clay/$LiClO_4$ Systems

HSIEN-WEI CHEN, CHUN-YI CHIU, FENG-CHIH CHANG

Institute of Applied Chemistry, National Chiao-Tung University, Hsin-Chu, Taiwan 30043, China

Received 21 December 2001; revised 18 February 2002; accepted 10 April 2002

ABSTRACT: This study demonstrates that adding clay that was organically modified by dimethyldioctadecylammonium chloride (DDAC) and d2000 surfactants increases the ionic conductivity of polymeric electrolyte. A.C. impedance, differential scanning calorimetric (DSC), and Fourier transform infrared (FTIR) studies revealed that the silicate layers strongly interact with the dopant salt lithium perchlorate ($LiClO_4$) within a poly(ethylene oxide) (PEO)/clay/$LiClO_4$ system. DSC characterization verified that the addition of a small amount of the organic clay reduces the glass-transition temperature of PEO as a result of the interaction between the negative charge in the clay and the lithium cation. Additionally, the strength of such a specific interaction depends on the extent of PEO intercalation. With respect to the interaction between the silicate layer and the lithium cation, three types of complexes are assumed. In complex I, lithium cation is distributed within the PEO phase. In complex II, lithium cation resides in an PEO/exfoliated-clay environment. In complex III, the lithium cation is located in PEO/agglomerated-clay domains. More clay favors complex III over complexes II and I, reducing the interaction between the silicate layers and the lithium cations because of strong self-aggregation among the silicate layers. Notably, the $(PEO)_8LiClO_4$/DDAC-modified clay (DDAC-mClay) composition can form a nanocomposite electrolyte with high ionic conductivity (8×10^{-5} S/cm) at room temperature. © 2002 Wiley Periodicals, Inc. J Polym Sci Part B: Polym Phys 40: 1342–1353, 2002

Keywords: polymeric electrolytes; clay; FTIR; nanocomposite

INTRODUCTION

Developing solid polymer electrolytes (SPEs) with a high ionic conductivity at room temperature has received considerable attention in recent years.[1–8] Such efforts focus mainly on applying the electrolytes to rechargeable and high-energy density power sources. As widely believed, lithium-based electrochemical systems can be configured to the battery.[2,9–14] Various efforts have been made to design new polymeric matrices by synthetic processes or modifying existing polyether-salt complexes, and thus improve ionic conductivity.[15–21] Introducing nanosized inorganic fillers is a successful method.[9,22–24] Clay mineral is an inorganic filler with intercalating properties. An intercalating polymer within a layered clay host provides a polymer electrolyte nanocomposite with a huge interfacial area. The higher interfacial area reduces the crystallinity of polyether chains, increasing the ionic conductivity. Furthermore, the mechanical properties of this semicrystalline poly(ethylene oxide) (PEO)-based electrolyte can also be improved. From our previous research,[25,26] the incorporation of the appropriate quantity of clay can drastically increase the ionic conductivity. This clay mineral can dissolve lithium cations because these silicate layers of the clay play the role of a Lewis base to complex with the lithium cations. However, the effect of polymer intercalation with the clay on the ionic con-

Correspondence to: F.-C. Chang (E-mail: changfc@cc.nctu.edu.tw)

Journal of Polymer Science: Part B: Polymer Physics, Vol. 40, 1342–1353 (2002)

ductivity enhancement is not clearly understood. A model system based on PEO doped with lithium perchlorate ($LiClO_4$) and in which various organic modified clays are incorporated is examined in this work. Furthermore, the intercalating effect of the clay on the polymer electrolyte is detected using X-ray diffraction, differential scanning calorimetry (DSC), and Fourier transform infrared spectroscopy (FTIR).

EXPERIMENTAL

Materials

Sample Preparation

The PEO with a weight-average molecular weight (M_w) of 200,000 was purchased from Aldrich. $LiClO_4$ also purchased from Aldrich was dried in a vacuum oven at 80 °C for 24 h and then stored in a desiccator prior to use. Acetonitrile was refluxed at a suitable temperature under nitrogen atmosphere prior to use. Dimethyldioctadecylammonium chloride (DDAC) was purchased from Aldrich. Poly(oxypropylene) diamine [the trade name is d2000, number-average molecular weight (M_n) = 2000] was purchased from Huntsman Co. (United States). DDAC and d2000 are used to modify the clay, and the structures are illustrated in Structure 1.

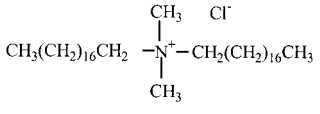

DDAC

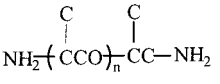

d2000

Preparation of Mineral Clay

DDAC-Modified Clay The process of modifying the clay was carried out according to the literature.[23] The cation-exchange capacity of sodium montmorillonite was 1.15 meq/g. The clay, sodium montmorillonite (1 g), and 50 mL of distilled water were placed in a 100-mL beaker, and 1 g of dimethyldioctadecylammonium chloride was added to the solution. The mixture was stirred vigorously for 8 h, filtered, and then washed three times with 100 mL of hot water to remove NaCl. After washing with ethanol (50 mL) to remove residual ammonium salt, the modified clay was dried in a vacuum oven at 60 °C for 24 h. See the following:

DDAC-clay: M_w of DDAC = 585.5 (g/mol) [585.5 $\times$ 1.15 $\times$ 10^{-3} = 0.673 g (DDAC required)] and M_w of NaCl = 58.5 (g/mol) [58.5 $\times$ 1.15 $\times$ 10 -3 = 0.0673 g (NaCl produced)].

d2000-Modified Clay Half-mole of the d2000 diamine was acidified by hydrochloric acid (HCl). The clay, sodium montmorillonite (1 g), and 50-mL distilled water were placed in a 100-mL beaker, and 2.3 g of acidified d2000 was added to the solution (Clay/d2000 = 1/1). The mixture was stirred vigorously for 8 h, filtered, and then washed with deionized water. The modified clay was dried in a vacuum oven at 60 °C for 24 h. Notably, the D-2000 modified montmorillonite is highly hydrophobic as seen in the following:

d2000-clay: M_w of d2000 = 2000 (g/mol) [2000 $\times$ 1.15 $\times$ 10^{-3} = 2.3 g (d2000 required)] and M_w of NaCl = 58.5 (g/mol) [58.5 $\times$ 1.15 $\times$ 10^{-3} = 0.0673 g (NaCl produced)].

Preparation of Solid Polymer Electrolyte (SPE)

A Desired amount of PEO, vacuum-dried $LiClO_4$ salt, and the clay in dry acetonitrile were mixed to form PEO/clay/$LiClO_4$ nanocomposites of various compositions. Following continuous stirring for 24 h at 80 °C, these solutions were maintained at 50 °C for an additional 24 h to facilitate initial desolvent. Further drying was carried out under vacuum at 70 °C for 3 days. To prevent contact with air and moisture, all nanocomposites prepared were stored in a drybox filled with nitrogen. All samples were allowed to equilibrate at ambient temperature for at least 1 month in a drybox before undertaking any additional experiment.

Methods

X-ray Measurements

Wide-angle X-ray diffraction experiments were conducted on a Rigaku X-ray diffractometer using the Cu Kα radiation (18-kw rotating anode, λ = 1.5405 Å) at 50 kv and 250 mA with a scanning rate of 2°/min.

DSC

Thermal behaviors of PEO-based electrolyte films were characterized by a DSC instrument from DuPont (DSC-9000) equipped with a low-temperature measuring head and a liquid nitrogen-cooled heating element. About 3–6 mg of sample in an aluminum pan were stabilized by slow cooling to −110 °C and then heated at 10 °C/min to 200 °C.

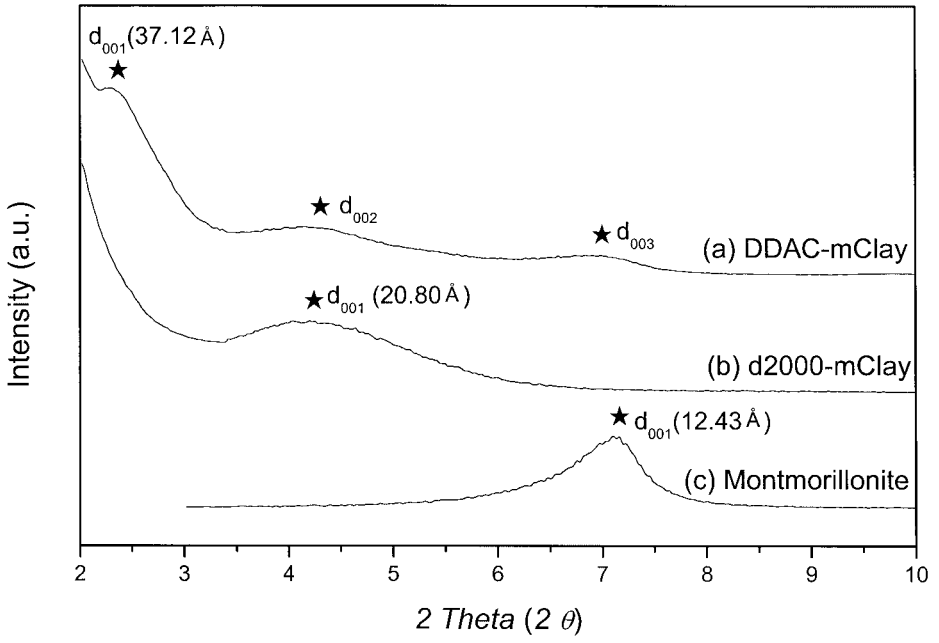

Figure 1. XRD patterns of organophilic clays: (a) DDAC-mClay, (b) d2000-mClay, and (c) plain-Clay.

FTIR Measurements

The conventional NaCl disk method was used to measure infrared spectra of composite films. All polymer films were prepared within N_2 atmosphere. The acetonitrile solution was cast onto a NaCl disk from which the solvent was removed under vacuum at 70 °C for 48 h. All infrared spectra were obtained at a resolution of 1 cm^{-1} on a Nicolet AVATAR 320 FTIR spectrometer at 120 °C.

Conductivity Measurements

Ionic conductivity measurements with alternating current were conducted on a AUTOLAB designed by Eco Chemie within the frequency range from 10 MHz to 10 Hz. The composite film was sandwiched between two stainless steel blocking electrodes (1-cm diameter). The specimen thickness varied from 0.8 to 1.2 mm, and the impedance response was gauged over the range from 20 to 120 °C.

RESULTS AND DISCUSSION

Organic Modified MMT

The surface layer of hydrophilic Na montmorillonite (MMT) was modified by dispersing MMT uniformly in an organic modifier solution. Consequently, the surface of MMT had a hydrophobic character.[27,28] The hydrophobic organic modifier facilitates the intercalation of a hydrophobic polymer into MMT by reducing the surface energy. The cation-exchange capacity of MMT in this study was 1.15 meq/g. Therefore, 1 g of MMT requires 0.673 g of DDAC (M_w = 585.5 g/mol) to stoichiometrically exchange sodium cations to produce 0.0673 g of NaCl. Similarly, 1 g of MMT requires 2.3 g of d2000 (M_w = 2000 g/mol) to exchange sodium cations and produces 0.0673 g of NaCl. (0.5 mol of d2000 diamine was acidified with HCl before cation exchange proceeded.). Eventually, the organic modified clay was washed by water removing the NaCl.

The clay was treated organically with DDAC and d2000 separately to examine the effect of the modified MMT on the morphology of PEO/clay nanocomposite. The interlayer spacing was determined from the X-ray diffraction (XRD) peak using the Bragg equation

$$\lambda = 2d\sin\theta$$

where d corresponds to the spacing between diffractional lattice planes, θ is the diffraction position, and λ is the wavelength of the X-ray (1.5405 Å). Figure 1 displays XRD patterns of organophobic clays. In the d2000-modified (d2000-mClay) and DDAC-modified clay (DDAC-mClay) systems, the basal interlayer spacing increased from 12.43 to 20.8 and 37.12 Å, respectively. This result

clearly demonstrated that the interlayer spacing of silicate layers increases with the insertion of DDAC and d2000 by ion exchange.

PEO/Clay Nanocomposites

The effect of organic modifiers on the intercalating behavior of the polymer can also be confirmed by an XRD pattern. As would be expected, the intercalation of the polymer chains further increases the interlayer spacing of the clay over that of pure clay, shifting the diffraction peak toward lower θ. Various compositions of PEO/clay have been prepared to produce PEO/clay nanocomposites. Figure 2 presents XRD patterns recorded at room temperature for (a) PEO/DDAC-mClay, (b) PEO/d200-mClay, and (c) PEO/plain-Clay. Table 1 summarizes the results. As shown in Figure 2(a), no basal peak (ranging from 2 to 3°) can be detected from hybrids with 2.9 and 5.7% DDAC-mClay. This fact reveals that clays in both composites are exfoliated and dispersed homogeneously within the PEO matrix. However, basal interlayer spacing appears at a higher clay content (>5.7%), and this diffractional peak shifts toward a higher angle as the clay concentration increases, indicating a lower interlayer spacing between silicate layers. This phenomenon can be attributed to fewer polymer chains intercalating within the silicate galleries. Adding more hydrophilic clay increases the hydrophilicity and reduces the compatibility between the clay and the hydrophobic polymer, increasing agglomeration among these silicate layers. Notably, the composition with 2.9% DDAC-mClay in the PEO/clay system can produce the nanocomposite with a huge number of silicate layers dispersed uniformly in the PEO matrix.

The PEO/d2000-mClay series exhibits the same trend [Fig. 2(b)]. The basal interlayer spacing increases as PEO chains are inserted into the silicate galleries, and the interlayer spacing (23.99 Å) is maximum at 2.9% clay. Furthermore, the interlayer spacing declined as the clay content increased. Polymer intercalation in the PEO/d2000 series seems not as apparent as in the PEO/DDAC-mClay series. Figure 2(c) shows the intercalating property of the PEO/plain-Clay system when the clay is not organically modified. The basal interlayer spacing increases when the clay is blended with the polymer. Nevertheless, the diffractional peak is not obviously shifted by varying the clay content in the PEO/clay hybrid. The lake of an increase in the interlayer spacing is attributed to the incompatibility between the polymer and the clay. The hydrophobic polymer chains cannot enter the silicate galleries because of the high hydrophilicity of the silicate layer. The clay platelets are difficult to be dispersed homogeneously in the polymer matrix and tend to form large aggregates resulting in phase separation. The XRD results indicate that the clays organically modified by DDAC and d2000 can increase the compatibility between the clay and the polymer. Furthermore, the PEO/DDAC-mClay can produce more silicate layers in the PEO matrix than in PEO/d2000-mClay because of the higher compatibility between PEO and the clay.

DSC Studies

Pertinent literature[9,29–31] has conferred that PEO can complex with the $LiClO_4$ salt, following the Lewis base–acid-type interaction between the polyether matrix and lithium cations. This strong Lewis base–acid interaction formats the transient crosslinks between the salt and the polyether phase. DSC analysis is generally one of the most convenient methods for estimating the mobility of the polyether chain. Figure 3 presents conventional second-run DSC thermograms of PEO/clay/$LiClO_4$ ternary blends that contain a specific content of $LiClO_4$ (EO/Li^+ = 8). In the $(PEO)_8LiClO_4$/DDAC-mClay system [Fig. 3(a)], the glass-transition temperature (T_g) declines as the clay content increases and reaches a minimum when the clay concentration is 1%. Subsequently, T_g increases dramatically with a further increase of the clay concentration. However, neither $(PEO)_8LiClO_4$/d2000-mClay nor $(PEO)_8LiClO_4$/plain-Clay systems follows a similar trend. In the $(PEO)_8LiClO_4$/d2000-mClay system [Fig. 3(b)], the T_g declines progressively as the clay content is increased. However, the T_g increases gradually when the plain-Clay is added into the $(PEO)_8LiClO_4$ system [Fig. 3(c)]. Figure 4 plots T_g versus clay content (%) for various organic clay systems. T_g for pure PEO is −67 °C, whereas T_g of $(PEO)_8LiClO_4$ is −14 °C. T_g declines dramatically from −14 to −55 °C when 1% of DDAC-mClay is added. Subsequently, T_g increases drastically as the clay content is increased to 9.1% and eventually levels off at 16.7%. The decrease in T_g is caused by the weakening of the salting effect when the clay is incorporated. Restated, adding clay can reduce the interaction between ether groups and lithium cations. This observed trend in T_g can be interpreted as Lewis base–acid-type interactions among the polyether matrix, the clay filler, lithium cations, and corresponding anions. Figure 5

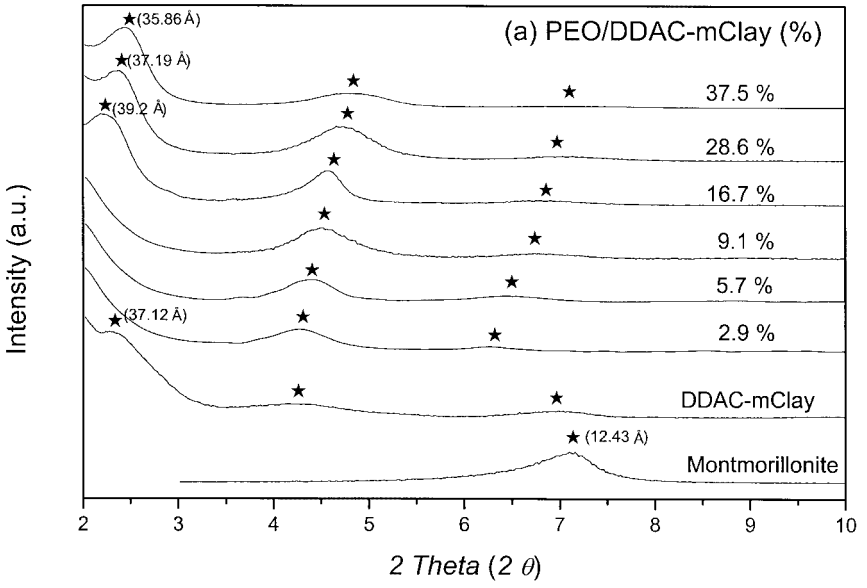
(a) PEO/DDAC-mClay (%)
★(35.86 Å)
★(37.19 Å)
★(39.2 Å)
37.5 %
28.6 %
16.7 %
9.1 %
5.7 %
★(37.12 Å)
2.9 %
DDAC-mClay
★(12.43 Å)
Montmorillonite
Intensity (a.u.)
2 Theta (2 θ)

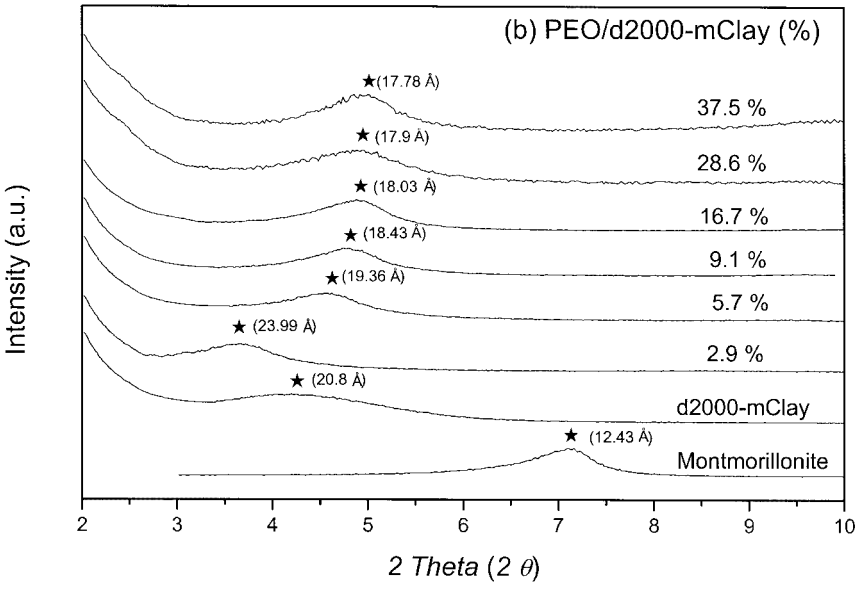
(b) PEO/d2000-mClay (%)
★(17.78 Å)
37.5 %
★(17.9 Å)
28.6 %
★(18.03 Å)
16.7 %
★(18.43 Å)
9.1 %
★(19.36 Å)
5.7 %
★(23.99 Å)
2.9 %
★(20.8 Å)
d2000-mClay
★(12.43 Å)
Montmorillonite
Intensity (a.u.)
2 Theta (2 θ)

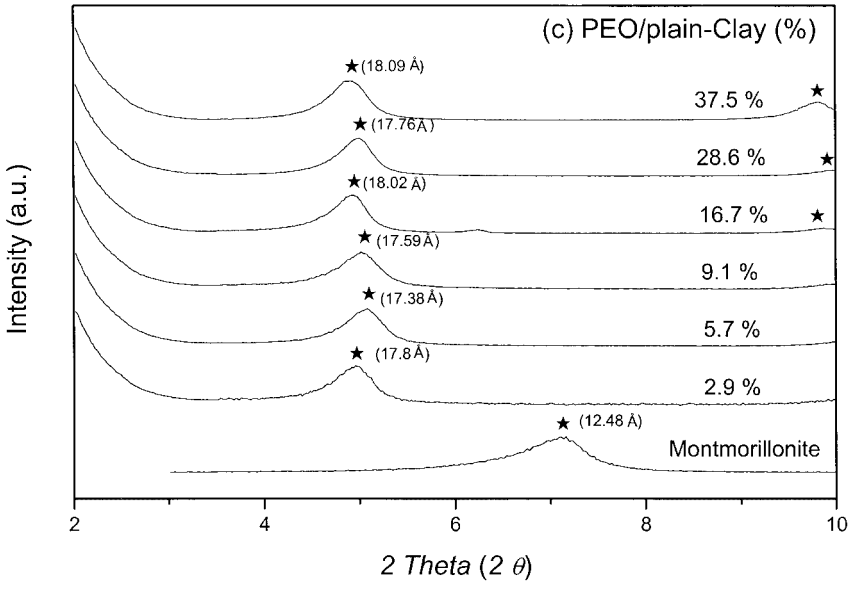
(c) PEO/plain-Clay (%)
★(18.09 Å)
37.5 %
★(17.76 Å)
28.6 %
★(18.02 Å)
16.7 %
★(17.59 Å)
9.1 %
★(17.38 Å)
5.7 %
★(17.8 Å)
2.9 %
★(12.48 Å)
Montmorillonite
Intensity (a.u.)
2 Theta (2 θ)

Table 1. Basal Spacing d_{001} (Å) after Calcinations at Different Organomodified

	Basal Spacing d_{001} (Å)		
Composition (%)	DDAC-mClay	d2000-mClay	Plain-Clay
Organic modified	37.12	20.80	—
2.9	41.17[a]	23.99	17.80
5.7	40.38[a]	19.36	17.38
9.1	39.29[a]	18.43	17.59
16.7	39.20	18.03	18.02
28.6	37.19	17.90	17.76
37.5	35.86	17.78	18.09

[a] The value was calculated by the double spacing d_{002}.

depicts these specific interactions for these three types of complexes. The first type of interaction, complex I, complexes between the PEO and the lithium cations. The second type of interaction, complex II, complexes among PEO, exfoliated clay, and lithium cations. The third type of interaction, complex III, involves lithium cations, PEO, and the agglomerated clay. The PEO/$LiClO_4$ system that does not contain the clay can form only complex I. Some of complex I tends to be converted into complex II when the composite contains the exfoliated clay because Li^+ cations strongly interact with silicate layers. Our prior studies[25,26] reveal that the silicate layers act as a Lewis base because the negative charges in the clay surface can complex with lithium cations. When these silicate layers are exfoliated, many such negative charges in the clay favor complexing with the lithium cations. XRD results (Table 1) show that the PEO/DDAC-mClay composite with a relatively lower organoclay content (<5.7%) has a high interlayer spacing, indicating an exfoliated structure. Some of the original lithium cations in complex I are drawn into the clay region to form complex II. Such transitions increase the flexibility of the PEO chain and thus reduce T_g. However, a higher clay content favors the formation of complex III and reduces the interaction between silicate layers and lithium salts because of the strong self-aggregation among these silicate layers. Meanwhile, the ether group has more chances to clutch the lithium cation leading to a higher PEO T_g. Self-aggregation not only reduces the probability of interaction between silicate layers and lithium cations but also creates a steric hindrance that retards the chain mobility. In this system, two adverse and competitive effects are present; one favors lower T_g (Lewis base–acid interaction), and the other favors higher T_g (steric effect of clay agglomeration). A decreased T_g with incorporation of clay concentration is also observed in the $(PEO)_8LiClO_4$/d2000-mClay system. As would be expected, a lower clay interlayer spacing (lower surface area of silicate layers) requires a higher clay content to provide sufficient negative charges to attract a particular quantity of lithium cations. Consequently, the $(PEO)_8LiClO_4$/d2000-mClay system requires a higher clay content to draw an equal amount of lithium cations away from the PEO region because of the lower expandability of the clay. However, the critical clay concentration of the lowest T_g was not found in this system, and we suspect that the critical clay concentration may exceed 37.5% clay. The plain-Clay system exhibits the opposed trend; the T_g increases slightly as the content of untreated clay increases. This behavior is attributable to the strong agglomeration among the silicate layers (complex III) and the fact that the unfavorable effect (steric hindrance) dominates the favorable effect (draw Li^+ into the clay region), even with a small quantity of the clay. Therefore, T_g of PEO increases steadily with clay content.

FTIR Spectroscopy

FTIR spectroscopy is a powerful tool for probing microscopic details of electrolytic systems. The

Figure 2. XRD patterns of PEO/clay hybrids containing various organophilic clay concentrations (%): (a) PEO/DDAC-mClay system, (b) PEO/d2000-mClay system, and (c) PEO/plain-Clay system.

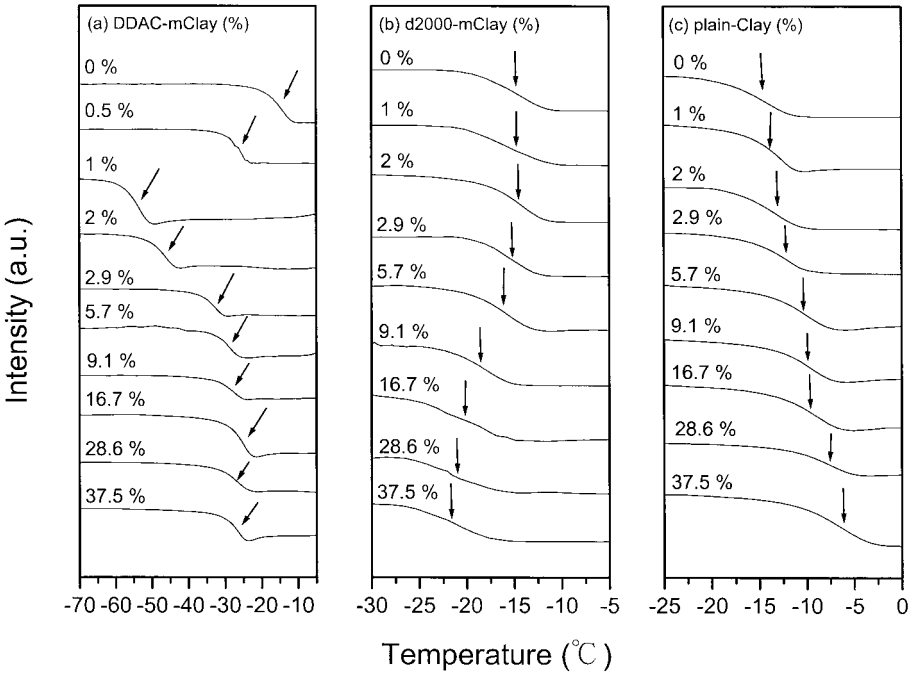

Figure 3. DSC traces obtained for $(PEO)_8LiClO_4$/clay composite electrolytes containing various organophilic clay concentrations (%): (a) $(PEO)_8LiClO_4$/DDAC-mClay system, (b) $(PEO)_8LiClO_4$/d2000-mClay system, and (c) $(PEO)_8LiClO_4$/plain-Clay system.

characteristic $\nu(ClO_4^-)$ mode of $LiClO_4$ is particularly sensitive in changing the local anionic environment.[14,32–34] Relevant studies[14,34] claim that the adsorption band observed at ~624 cm^{-1} corresponds to the "free" anion that does not interact directly with the lithium cations. The adsorption

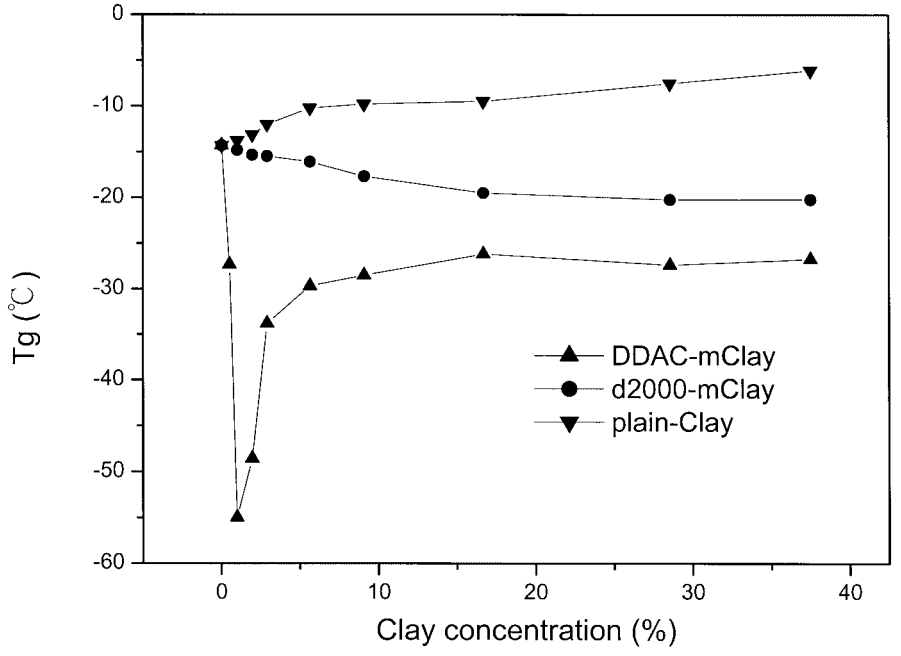

Figure 4. T_g versus organophilic clay concentration (%) for $(PEO)_8LiClO_4$/clay composite electrolytes: (▲) $(PEO)_8LiClO_4$/DDAC-mClay system, (●) $(PEO)_8LiClO_4$/d2000-mClay system, and (▼) $(PEO)_8LiClO_4$/plain-Clay system.

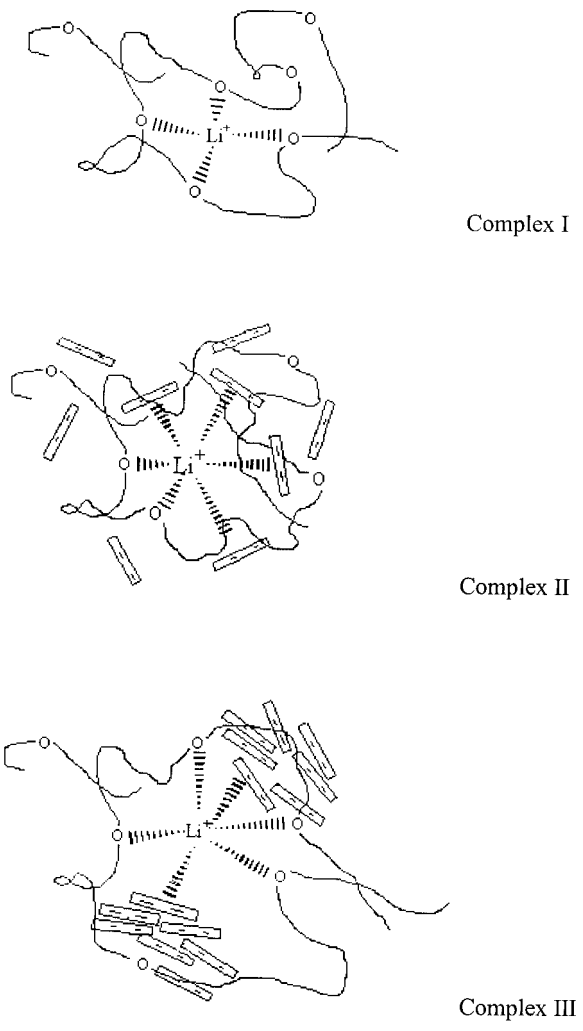

Figure 5. Structure of the complex formed by Li^+ cation with (a) polyether chains (complex I), (b) polyether and well-exfoliated silicate layers (complex II), and (c) polyether and self-agglomerated silicate layers (complex III).

band at ~635 cm^{-1} has been attributed to the contact ion pair. Figure 6 illustrates typical infrared spectra for $\nu(ClO_4^-)$ between 650 and 600 cm^{-1}, recorded at 120 °C for PEO/$LiClO_4$/clay ternary blends that contain a constant $LiClO_4$ concentration ($EO/Li^+ = 8$) and various organic clay contents. As shown in Figure 6(a), the shoulder of the ion pair (~635 cm^{-1}) decreases gradually as the DDAC-mClay content increases and eventually disappears when the DDAC-mClay content is 9.1%. When the DDAC-mClay content is further increased above 9.1%, the intensity of the shoulder increases again and gradually approaches its original value. However, the chemical shift of the "free" anion at 624 cm^{-1} can also be observed when DDAC-mClay is added. The band of "free" anion (624 cm^{-1}) shifts to a lower wave number when a little DDAC-mClay is added. However, this band also returns to the original wave number when more DDAC-mClay is added. The change of the intensity of the ion pairs band (~ 635 cm^{-1}) and the chemical shift of the "free" anion (~624 cm^{-1}) indicate that these electrons that surround the lithium cation are deprived by adding DDAC-mClay. Restated, the attractive force between the lithium cation (Li^+) and anion (ClO_4^-) is reduced by the presence of the negative charge in silicate layers. The $(PEO)_8LiClO_4$/d2000-mClay system exhibits the same trend [Fig. 6(b)]. The band of the ion pair decreases as the d2000-mClay increases, and the minimum intensity is observed when the d2000-mClay content is 16.7%. When the d2000-mClay content is increased to 16.7% or higher, the intensity of the shoulder increases almost to its original value. However, the change in the intensity of the ion pair is also accompanied by the chemical shift of the "free" anion band (~624 cm^{-1}). Figure 6(c) shows the $\nu(ClO_4^-)$ spectral stretch of the $(PEO)_8LiClO_4$/plain-Clay system for various clay contents. No obvious change in the intensity (~635 cm^{-1}) or the chemical shift (624 cm^{-1}) can be observed, revealing the absence of specific interaction between lithium salts and silicate layers.

The fractions of the "free" anion and ion pair shown in Figure 6 were measured by decomposing the $\nu(ClO_4^-)$ band into two Gaussian peaks. Figure 7 plots fraction of the "free" anion (%) against clay content (%) for the DDAC-mClay and d2000-mClay systems. The fraction of the "free" anion initially increases with the increase of the clay content and approaches a maximum at 9.1 and 16.7%, respectively. Subsequently, the fraction of the "free" anions decreases gradually as the clay content increases further. This observed trend in the fraction of "free" anion is consistent with the behavior of T_g, which is attributed to numerous Lewis base–acid-type interactions among the polyether matrix, the clay filler, lithium cations, and corresponding anions. The negative charges in the silicate layers similarly act as polar groups in PEO dissolving the lithium salt and influencing the charge environment of the anions. The capability for dissolution of anions depends on the contact area between the silicate layer and the lithium cation. The XRD results (Fig. 2) show that the PEO/DDAC-mClay composite yields a higher interlayer spacing than the PEO/d2000-mClay composite, indicating that the DDAC-mClay system can create more silicate lay-

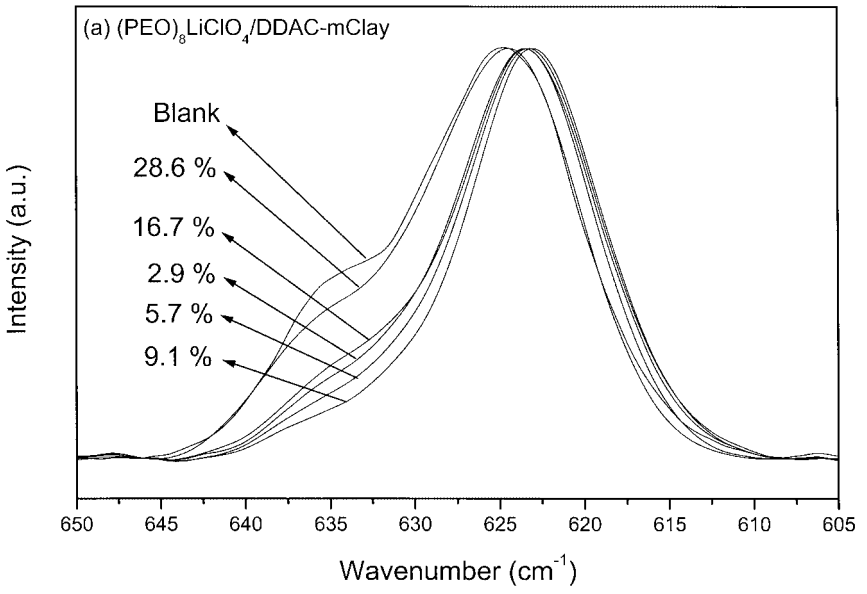
(a) (PEO)8LiClO4/DDAC-mClay
Blank
28.6 %
16.7 %
2.9 %
5.7 %
9.1 %
Intensity (a.u.)
650 645 640 635 630 625 620 615 610 605
Wavenumber (cm-1)

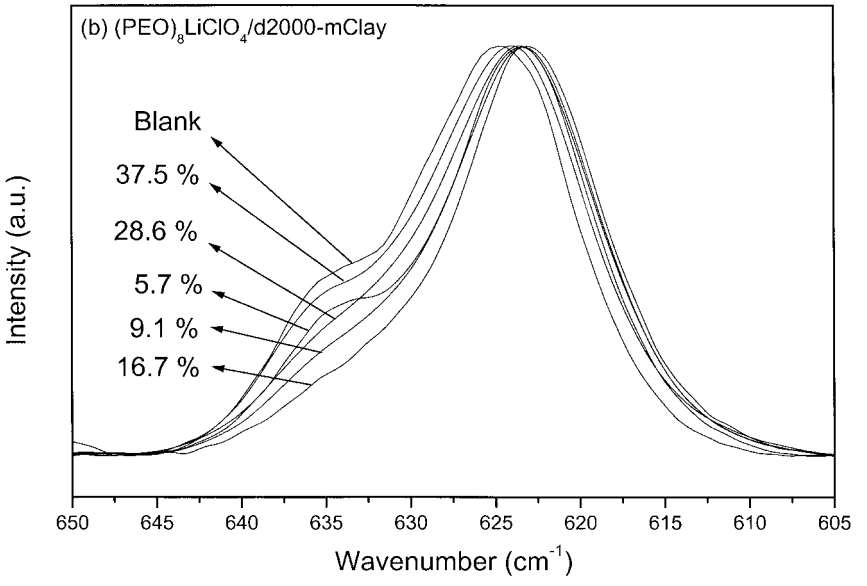
(b) (PEO)8LiClO4/d2000-mClay
Blank
37.5 %
28.6 %
5.7 %
9.1 %
16.7 %
Intensity (a.u.)
650 645 640 635 630 625 620 615 610 605
Wavenumber (cm-1)

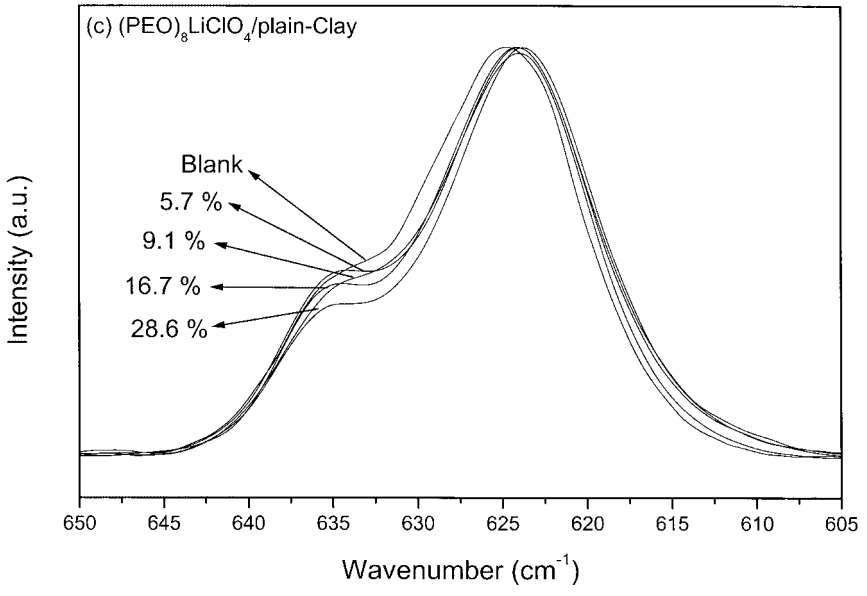
(c) (PEO)8LiClO4/plain-Clay
Blank
5.7 %
9.1 %
16.7 %
28.6 %
Intensity (a.u.)
650 645 640 635 630 625 620 615 610 605
Wavenumber (cm-1)

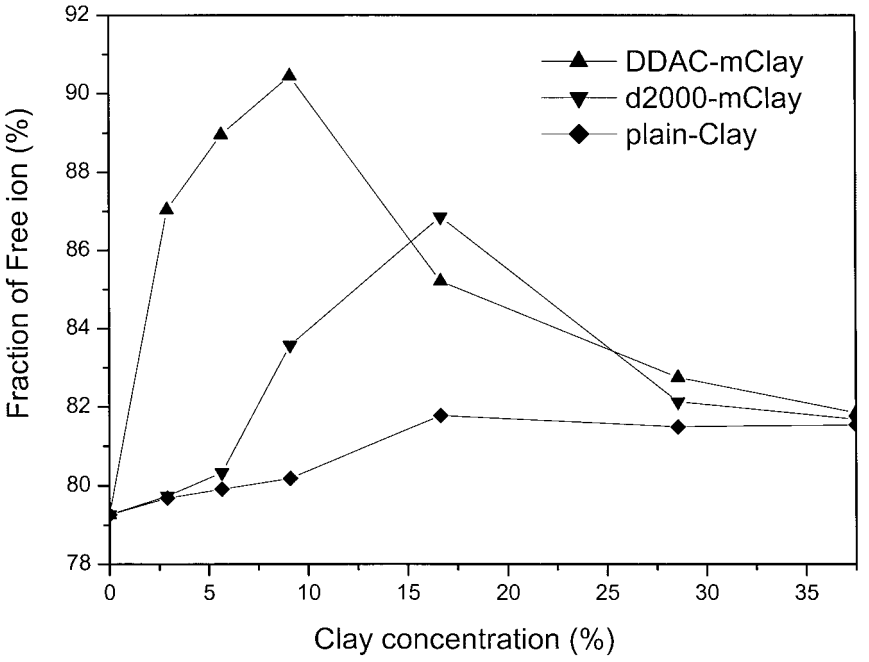

Figure 7. Fraction of "free" anions versus organophilic clay concentration (%) for $(PEO)_8LiClO_4$/clay composite electrolyte at 120 °C: (▲) $(PEO)_8LiClO_4$/DDAC-mClay system, (▼) $(PEO)_8LiClO_4$/d2000-mClay system, and (♦) $(PEO)_8LiClO_4$/plain-Clay system.

ers than the d2000-mClay system for a particular content. Consequently, the $(PEO)_8LiClO_4$/DDAC-mClay system requires less clay (9.1%) than the $(PEO)_8LiClO_4$/d2000-mClay system (16.7%) to dissolve a particular amount of lithium salt. However, the fraction of "free" anions declines to its original value as the clay increase further, implying that the silicate layer interacts less with lithium cations. The lower fraction of "free" anions at a high clay content is attributed to stronger self-aggregation among the silicate layers. Restated, the intraassociation of these silicate layers is favored over the interassociation of the silicate layer and the lithium cation at high clay content. Additionally, the fraction of "free" anion declines as the plain-Clay content increases, indicating that the interassociation is favored over the intraassociation as a result of the strong self-aggregation of the hydrophilic clays. The $\nu(ClO_4^-)$ spectral stretch is consistent with the XRD and DSC results. Adding clay not only influences the flexibility of the PEO chain but also impacts the charge environment of the lithium salt. However, the extent of the influence depends on the expandability of the clay.

Conductivity

Figure 8 plots conductivity versus clay content for the $(PEO)_8LiClO_4$/clay composite electrolytes at 30 °C. In the $(PEO)_8LiClO_4$/DDAC-mClay system, a rapid increase in the conductivity is observed when a small quantity of DDAC-mClay is added and the ionic conductivity is maximum at 2.9% clay concentration. At the clay concentration of above 2.9%, the ionic conductivity declines drastically and approaches its original value when the clay concentration is 23.1%. At a clay content above 23.1%, the conductivity further decreases even below the original value. The $(PEO)_8LiClO_4$/d2000-mClay system exhibits a similar trend, but the maximum ionic conductivity occurs at 16.7%

Figure 6. Infrared spectra of $\nu(ClO_4^-)$ internal modes for $(PEO)_8LiClO_4$/clay composite electrolytes containing various organophilic clay concentrations (%) at 120 °C: (a) $(PEO)_8LiClO_4$/DDAC-mClay system, (b) $(PEO)_8LiClO_4$/d2000-mClay system, and (c) $(PEO)_8LiClO_4$/plain-Clay system.

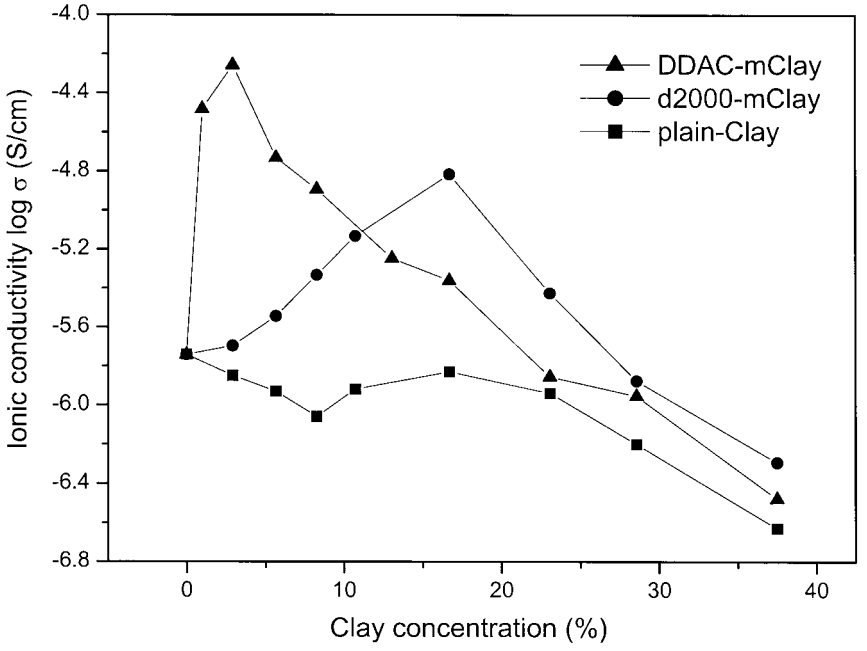

Figure 8. Ionic conductivity versus organophilic clay concentration (%) for $(PEO)_8LiClO_4$/clay composite electrolyte at 30 °C: (▲) $(PEO)_8LiClO_4$/DDAC-mClay system, (●) $(PEO)_8LiClO_4$/d2000-mClay system, and (■) $(PEO)_8LiClO_4$/plain-Clay system.

concentration. The conductivity also declines as the clay concentration is further increased. For the $(PEO)_8LiClO_4$/plain-Clay system, the ionic conductivity declines progressively as the clay content is increased.

The ionic conductivity (σ) of an electrolyte is defined as the product of the concentration of ionic charge carriers and their its mobility

$$\sigma = \sum_i n_i z_i \mu_i$$

where n_i, z_i, and μ_i refer to the number of charge carriers, the ionic charge, and the ionic mobility, respectively. According to the aforementioned equation, the ionic conductivity depends on the number of charge carriers (n_i) in the system and the mobility (μ_i) of the various species. The FTIR (Fig. 6) results indicate that adding a specific amount of organic clay results in the highest fraction of "free" anions and produces more charge carriers (higher n_i). However, more free charge carriers increase the ionic mobility (μ_i) because they disrupt the strong intraassociation between the lithium cations and anions. Consequently, the conductivity is expected to increase. In the $(PEO)_8LiClO_4$/d2000-mClay system, the conductivity increases to nearly eight times (8×10^{-6} S/cm) that of the $(PEO)_8LiClO_4$ plain electrolyte (1×10^{-6} S/cm) with 16.7% d2000-mClay. Notably, the highest conductivity (8×10^{-5} S/cm) is achieved when 2.9% DDAC-mClay is added to the $(PEO)_8LiClO_4$ system and is almost 45 times higher than that of the original $(PEO)_8LiClO_4$ system. This drastic increase in the conductivity of the $(PEO)_8LiClO_4$/DDAC-mClay system is attributed to the well-dispersed clay that tends to disrupt the intraassociation of lithium salt, increasing the number of freer charge carriers (n_i) and increasing ionic mobility (μ_i). However, an excess of clay mineral in the system may tightly hold the lithium cations and reduce ionic mobility, thereby reducing the observed conductivity. Thus, balanced interactions among the silicate layers, ether groups, lithium cations, and anions result in an optimum environment for ionic transport and achieve the highest possible ionic conductivity.

CONCLUSIONS

This study has demonstrated that the ionic conductivity of the $(PEO)_8LiClO_4$ system can be substantially enhanced by adding the optimal content of DDAC-mClay or d2000-mClay. A.C. impedance, DSC, and FTIR studies indicated that the silicate layer strongly interacts with the do-

pant salt $LiClO_4$ within a PEO/clay/$LiClO_4$ system. However, the strength of this specific interaction depends on the extent of PEO intercalation. In the exfoliated clay system, many negative charges are available in the silicate layers affecting the charge environment around the lithium anion and the mobility of the polymer matrix. A lower organic clay content favors the formation of complex II over complex I of the plain electrolyte by drawing Li^+ cations away from the PEO matrix. However, an excess of clay favors the formation of complex III as a result of strong self-aggregation among the silicate layers. Finally, the $(PEO)_8LiClO_4$/DDAC-mClay composition can form the nanocomposite electrolyte with a high ionic conductivity of 8×10^{-5} S/cm. This composition exhibits the potential for commercial applications.

REFERENCES AND NOTES

1. Scrosati, B. In Polymer Electrolyte Reviews; MacCallum, J. R.; Vincent, C. A., Eds.; Elsevier Applied Science: New York, 1989; p 315.
2. Scrosati, B. In Applications of Electroactive Polymers; Scrosati, B., Ed.; Chapman & Hall: New York, 1993; p 251.
3. Armand, M. B. Solid State Ionics 1983, 9/10, 745.
4. Chao, S.; Wrighton, M. S. J Am Chem Soc 1987, 109, 2197.
5. Fenton, D. E.; Parker, J. M.; Wright, P. V. Polymer 1973, 7, 319.
6. Ratner, M. A.; Shriver, D. F. Chem Rev 1988, 88, 109.
7. Wang, L.; Yang, B.; Wang, X. L.; Tang, X. Z. J Appl Polym Sci 1999, 71, 1711.
8. Wang, X. L.; Li, H.; Tang, X. Z.; Chang, F. C. J Polym Sci Part B: Polym Phys 1999, 37, 837.
9. Wieczorek, W.; Raducha, D.; Zalewska, A.; Stevens, J. R. J Phys Chem B 1998, 102, 8725.
10. Abraham, K. M.; Jiang, Z.; Carroll, B. Chem Mater 1997, 9, 1978.
11. Yang, X. Q.; Hanson, L.; McBreen, J.; Okamoto, Y. J Power Sources 1995, 54, 198.
12. Lee, J. C.; Litt, M. H. Macromolecules 2000, 33, 1618.
13. Labreche, C.; Levesque, I.; Prud'homme, J. Macromolecules 1996, 29, 7795.
14. Mishra, R.; Rao, K. J. Solid State Ionics 1998, 106, 113.
15. Allcock, H. R.; Prange, R.; Hartle, T. J. Macromolecules 2001, 34, 5463.
16. Allcock, H. R.; Laredo, W. R.; Clay Kellam, E., III.; Morford, R. V. Macromolecules 2001, 34, 787.
17. Chen-Yang, Y. W.; Hwang, J. J.; Huang, A. Y. Macromolecules 2000, 33, 1237.
18. Allcock, H. R.; Sunderland, N. J.; Ravikiran, R.; Nelson, J. M. Macromolecules 1998, 31, 8026.
19. Mertens, I. J. A.; Wübbenhorst, M.; Oosterbaan, W. D.; Jenneskens, L. W.; van Turnhout, J. Macromolecules 1999, 32, 3314.
20. Wen, T. C.; Luo, S. S.; Yang, C. H. Polymer 2000, 41, 6755.
21. Wen, T. C.; Wang, Y. J.; Cheng, T. T.; Yang, C. H. Polymer 1999, 40, 3979.
22. Scanlon, L. G.; Giannelis, E. P. Adv Mater 1995, 7, 154.
23. Ogata, N.; Kawakage, S.; Ogihara, T. Polymer 1997, 38, 5115.
24. Croce, F.; Appetecchi, G. B.; Persi, L.; Scrosati, B. Nature 1998, 394, 456.
25. Chen, H. W.; Chang, F. C. Polymer 2001, 42, 9763.
26. Chen, H. W.; Chang, F. C. J Polym Sci Part B: Polym Phys 2001, 39, 2407.
27. Lan, T.; Pinnavaia, T. J. Chem Mater 1994, 6, 2216.
28. Lan, T.; Kaviratna, P. D.; Pinnavaia, T. J. J Phys Chem Solids 1996, 57, 1005.
29. Li, J.; Khan, I. M. Macromolecules 1993, 26, 4544.
30. Li, J.; Pratt, L. M.; Khan, I. M. J Polym Sci Part A: Polym Chem 1995, 33, 1657.
31. Wieczorek, W.; Zalewska, A.; Raducha, D.; Florjanczyk, Z.; Stevens, J. R. J Phys Chem B 1996, 29, 143.
32. Xuan, X.; Wang, J.; Tang, J.; Qu, G.; Lu, J. Spectrochim Acta Part A 2000, 56, 2131.
33. Wang, Z.; Huang, B.; Huang, H.; Chen, L.; Xue, R. Solid State Ionics 1996, 85, 143.
34. Salomon, M.; Xu, M.; Eyring, E. M.; Petrucci, S. J Phys Chem 1994, 98, 8234.